Article ID: 1000-324X(2011)09-1003-06 **DOI:** 10.3724/SP.J.1077.2011.11135

Bimodal Distribution of Microstructure and Mechanical Properties of Plasma Sprayed Nanostructured Al_2O_3-13wt% TiO_2 Coatings

LU Xue-Cheng[1,2], YAN Dian-Ran[1], YANG Yong[1], HE Ji-Ning[1], ZHANG Jian-Xin[1], DONG Yan-Chun[1]

(1. Key Lab for new type of functional materials in Hebei Province, Hebei University of Technolgy, Tianjin 300130, China; 2. Handing Equipment Mechanical Department, Military Transportation University, Tianjing 300161, China)

Abstract: Nanostructured Al_2O_3-13wt% TiO_2 coatings were prepared by plasma spraying agglomerated nanocrystalline powders formed *via* spray drying method. The phase composition, microstructure, microhardness and fracture toughness of the coatings were investigated. It is found that the nanostructured coatings exhibited a unique bimodal microstructure consisting of two distinct regions: one of the regions is Fully Melted (FM) and solidified as lamellar structure, and the other is Partially Melted (PM) particulate microstructure with embedded nano or sub-micron particles retained from the starting powders. Furthermore, the percentage of PM region, which is proportional to unmelted α-Al_2O_3 nanoparticles, in the coatings can be controlled by the critical plasma spray parameter. Such a characteristic of blended microstructure of the coatings is clearly confirmed from a bimodal distribution of their mechanical properties. The Weibull statistical analysis shows that the microhardness and fracture toughness of the coatings present a bimodal distribution, the mean value and the dispersity of microhardness of PM region are lower than those of FM region, but the mean value and the dispersity of fracture toughness of PM region are both higher than those of FM region.

Key words: plasma spraying; nanostructure coatings; microstructure; mechanical properties; bimodal distribution

Plasma sprayed ceramic coatings have been developed with outstanding properties[1-3]. Proper deposition of nanostructure plasma sprayed ceramic coatings, by taking advantage of properties associated with nanostructures, can provide an advancement in the performance and durability of conventional plasma sprayed coatings that already have a wide variety of applications. It has been previously demonstrated that many excellent properties such as improved wear resistance, adhesion strength, spallation resistance during bend- and cup-tests, and indentation crack resistance can be attained by the controlled deposition of nanostructure Al_2O_3-13wt% TiO_2 agglomerated powder using plasma spray techniques[2-4].

In the present work, nanostructured Al_2O_3-13wt% TiO_2 coatings were prepared by atmosphere plasma spraying nanocrystalline powders, the constituent phases and the microstructure of the coatings were examined in detail by a number of characterization techniques. Based on the investigation of the microstructure, the bimodal distribution of the microhardness and fracture toughness of the coatings were analysed by means of Weibull statistical analysis, thus the effect of microstructure on the properties of the as-sprayed nanocoatings were further discussed.

1 Experimental Procedure

1.1 Preparation of coatings

Commercial nanosized α-Al_2O_3 and rutile TiO_2 powders used as the raw materials have a mean diameter of 50nm and 20nm, respectively. The sprayable micrometer-sized agglomerated powders were prepared by spray drying the blended slurry with composition of Al_2O_3-13wt% TiO_2, and subsequently sintered in the temperature range of 1000–1200℃. SEM image and line scanning of the sprayable agglomerated powders are presented in Fig. 1. It can be seen that the agglomerated powders are spherical or ellipsoidal as shown in Fig. 1(a), which improve powders feeding behavior during plasma spraying process. Fig. 1(b) and (c) illustrate that the nanosized TiO_2 particles were homogeneously distributed among the Al_2O_3 particles.

The substrate samples with dimension of

Received date: 2011-03-07; **Modified date:** 2011-04-18; **Published online:** 2011-05-20
Foundation item: National Natural Science Foundation of China (51072045); Key Lab for New Type of Functional Materials in Hebei Province
Biography: LU Xue-Cheng (1978–), male, candidate of PhD. E-mail: luxuechengpla@yahoo.com.cn
Corresponding author: YAN Dian-Ran, professor. E-mail: yandianran@126.com

9mm×8mm×10mm, which were cut from carbon steel 45 named in China (composition; Fe-0.45C-0.3Si-0.75Mn-0.03P-0.035S(wt%)), were grit-blasted and then coated by plasma spraying Ni/Al powders to form as a bonding layer about 100 μm-thick. The nanostructure Al_2O_3-13wt% TiO_2 coatings were deposited by plasma spray using the agglomerated powders, and the coating thickness was about 300μm. The plasma spray was carried out on a LP-50B spray system as a function of a critical plasma spray parameter (CPSP) defined as[4]:

$$\text{CPSP} = \frac{\text{Voltage} \cdot \text{Current}}{\text{Primary Gas(Ar) Flow Rate}}$$

$$\text{(Unit: V·A/SCFH)} \qquad (1)$$

Other processing variables such as carrier gas flow rate, spray distance, flow rate ratio of Ar to H_2, powder feed rate, gun speed, *etc.*, were held constant in this study. Under these controlled processing conditions, CPSP can be directly related to the temperature of the plasma and/or the particles.

1.2 Characterization of coatings

The phase composition of the as-sprayed coatings was examined using PHILIPSX-PertMPD X-ray diffraction (XRD) with CuKα radiation. The microstructure was inspected using Philips XL30 scanning electron microscope (SEM) and PHILIPS TECNAI-F20 transmission electron microscope (TEM).

Microhardness values of the coatings were measured by digital hardness tester with load of 100g on the cross-section of the polished samples. The indentation fracture toughness test was performed on a digital Vickers hardness tester under a 1kg load, then the indentation crack length was measured. A rough estimate of fracture toughness can be made from the cracks emanating at the tip of the indentation using an empirical relationship[5]:

$$K_C = \chi\left(\frac{E}{H}\right)^{1/2}\frac{P}{a^{3/2}} \qquad (2)$$

where χ = 0.016, an empirical constant based on the indenter type and geometry; E is the elastic modulus about 300 GPa for the ceramic material; H is the hardness in GPa; P is the load applied in N; and a is the crack length in meters measured from the center of the indent.

The Weibull distribution analysis was used to evaluate the results of hardness and fracture toughness of the coatings.

2 Results and discussion

2.1 Phase composition analysis

The XRD patterns of the sprayable nanostructure Al_2O_3-13wt% TiO_2 agglomerated powders and as-sprayed coatings are shown in Fig. 2. As for the heat-treated nanostructure powders, Al_2O_3 retained the same α phase as the raw material, while TiO_2 changed from anatase to rutile due to an irreversible phase transition occurring at 610℃[3]. The results indicate that during plasma reprocessing, melting and partial melting of the nanostructure agglomerated powders occur, and they rapidly solidify to form metastable γ-Al_2O_3 from stable α-phase. Surprisingly, peaks of α-Al_2O_3 and γ-Al_2O_3 were found in XRD patterns from all as-sprayed coatings, however, peaks of the TiO_2 phase were not observed from as-sprayed coatings except for the coatings sprayed at the lower CPSP (*i.e.* 312) and only slight peaks of TiO_2 existed in the crystal planes (110), (101), (211). As mentioned by researchers[4], the solubility of TiO_2 in the equilibrium α-Al_2O_3 is negligible, Ti ions are likely to be in the γ-Al_2O_3 lattice as either an interstitial or substitutional defect. It has been reported that the plasma sprayed Al_2O_3-13wt% TiO_2 coatings contain non- equilibrium χ-Al_2O_3·TiO_2 phase in which Ti ions randomly occupy the Al^{3+} lattice sites in the γ-Al_2O_3 structure, and the peak positions of XRD for χ-Al_2O_3·TiO_2 phase are identical to those of γ-Al_2O_3, however the relative intensity of peaks are different[6-7]. The formation of χ-Al_2O_3·TiO_2 phase must originate from rapid liquid-to-solid transformation, which is expected during the plasma spray process and provides reasonable explanation for the absence of Ti-containing phase. Based on the above analysis, the missing of Ti-containing phase peaks can be attributed to the fact that, as the CPSP increases (along with particle/torch temperature), nanostructure TiO_2 is easier to be dissolved in γ-Al_2O_3 or

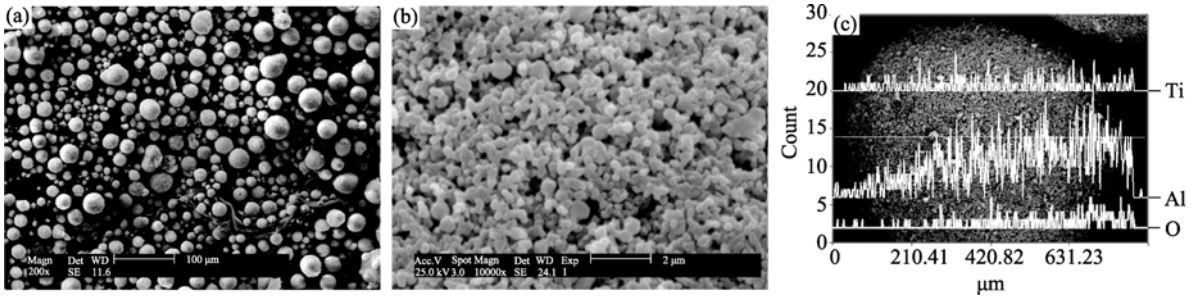

Fig. 1 Different magnification SEM images (a,b) of the agglomerated Al_2O_3-13wt% TiO_2 powders, and the line scanning result (c)

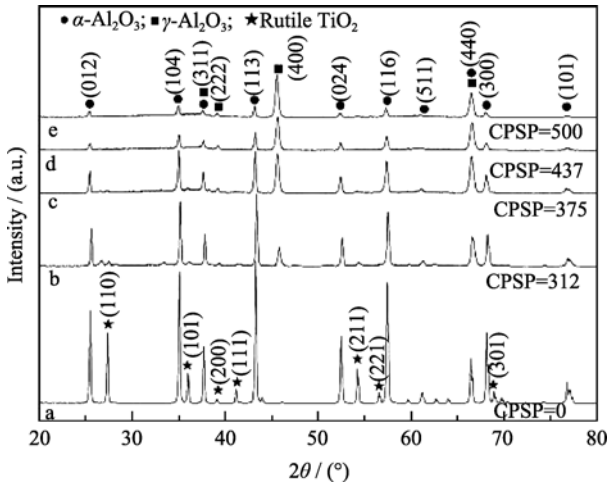

Fig. 2 XRD patterns for (a) nanostructure feedstock and (b, c, d, e) as-sprayed coatings

χ-Al_2O_3·TiO_2 phase presented in the nanocoatings, which is different from the investigation results of the conventional coatings as reported [1, 8].

It is evident that the phase composition of the coatings is sensitive to the CPSP of the plasma spray gun during production, as shown in Fig. 2. As the CPSP number increases, the relative ratio of integrated intensity from α-Al_2O_3 (113) to γ-Al_2O_3 (400) peaks ($I_{K_\alpha}^{\alpha(113)} / I_{K_\alpha}^{\gamma(400)}$) and the volume fraction of α-Al_2O_3 decreases, then γ-Al_2O_3 begins to dominate the microstructure. According to the results of XRD diffraction, the relative content of α-Al_2O_3 and γ-Al_2O_3 in nanostructured Al_2O_3-13wt%TiO_2 coating can be quantitatively calculated by direct *K* value method[4], as shown in Fig. 3.

Since melting and rapid solidification is the only processing route available for the formation of γ-Al_2O_3[9], it is clear that as CPSP increases (along with particle/torch temperature), the volume fraction of melted powder increases, conversely, the volume fraction of unmelted powders decrease. This bimodal distribution of melting state is expected to have favorable impact on microstructure and mechanical properties of the nanostructure coatings.

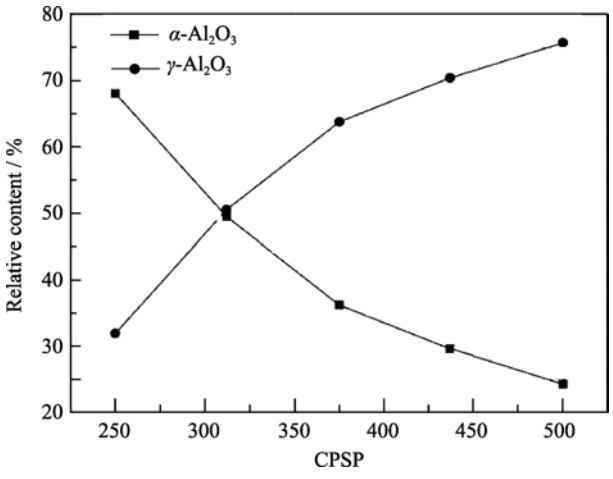

Fig. 3 Relative content of α-Al_2O_3 and γ-Al_2O_3 in nanostructure Al_2O_3-13wt%TiO_2 coating as a function of CPSP

2.2 Microstructure analysis

SEM images of plasma sprayed nanostructure Al_2O_3-13wt% TiO_2 coating are presented in Fig.4. As can be seen easily from Fig. 4(a), it is a typical lamellar microstructure, resulted from melting of the starting powders, impacting and well spreading on the substrate. The lamellar morphology was a nearly regular disk-like with limited splashing, indicating a rather good particle flattening and a strong bonding. The result was confirmed well from another point of view in Fig. 4(b) and Fig. 4(c).

The Al_2O_3-13wt%TiO_2 nanocoatings exhibited a particular bimodal microstructure consisting of two distinct regions as shown in Fig.4. One is a fully-melted (FM) region, where columnar grains (marked as A), skeleton-like structure (marked as B), and particulate reinforced solid solution type structure (marked as C) within lamellar splats are observed. The other is a partially-melted (PM) region, where some particulate microstructural features of the original powders are observed, and the microstructural features include sintered nano or sub-micron α-Al_2O_3 particles embedded in a matrix of Al_2O_3-TiO_2 matrix. In other words, the percentage of PM region is proportional to unmelted α-Al_2O_3 phase, so it can be controlled by the critical plasma spray parameter.

Figure 4(c) presents a quite different appearance of microstructure on the fracture surface, the splats in the nanostructured coating seem interlaced together and their boundaries as well as columnar grains are not so clearly identified as those in the conventional coating. There are some regions that appear rather rough and we assume that they are stemmed from the partially melted nanostructure particles, other regions look smooth, similar to the fractured facets in the conventional coating, which is considered corresponding to the fully melted regions in the coating.

In addition, it can be seen from Fig.4 that, the pores as one of the important part of the coatings also show bimodal distribution. The nearly spherical small closed pores (<3 μm) are typically caused by entrapped gases, most of the larger erose pores (>5 μm) are due to the formation of cavities at the boundaries of overlapping splats or retained from the starting hollow powders.

TEM also confirmed the bimodal microstructure, as presented in Fig. 5. It can be seen from Fig. 5(a) that, the equiaxed and bar-like grains exist in the fully melted region of the coating, the size of the equiaxed grains ranges

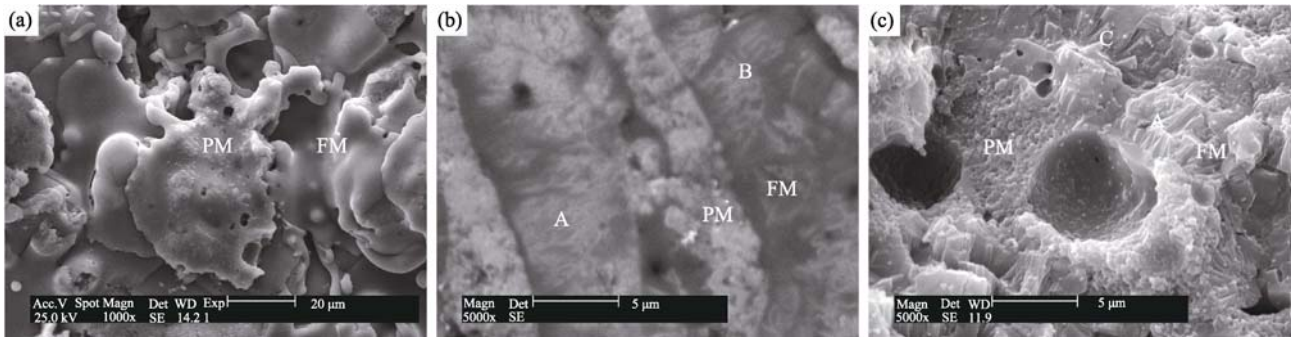

Fig. 4 SEM images of (a) surface , (b) cross-section and (c) fracture surface of plasma sprayed Al_2O_3-13wt%TiO_2 nanocoatings

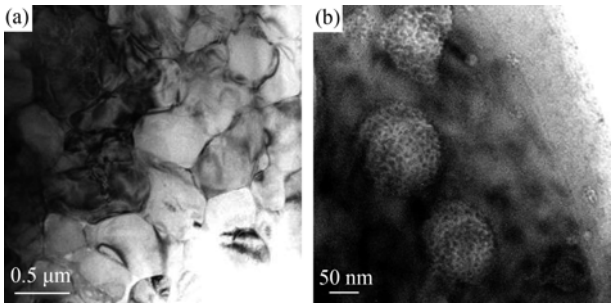

Fig. 5 TEM morphologies of (a) full melted region, and (b) partially melted region of plasma sprayed Al_2O_3-13wt%TiO_2 nanocoatings

from 80 to 200 nm, and the bar-like grains have a cross section in nanoscale and a length of several hundred nanometers. The boundaries of the grains are clearly defined, reflecting good bonding between grains. Some polygonal and irregular-shaped grains are also observed, which is believed to be the result of coalescence of smaller grains. Fig. 5(b) shows a TEM micrograph of PM region in the nanocoating, which indicates that some nanoparticles of about 70 nm in size embed in the matrix, corresponding to the morphology of area "C" in Fig. 4. As reported by researchers[9-10], the alumina transformation from liquid to γ-Al_2O_3 takes place preferentially due to a very high cooling rate and the low interfacial energy between γ-Al_2O_3 crystal and liquid , moreover, the melting point of alumina is higher than that of titania, so it is deduced that the nanoparticles belong to α-Al_2O_3 retained from unmelted Al_2O_3 starting powder, while the surrounding phase is amorphous and TiO_2 rich.

2.3 Mechanical properties of nanocoationgs

It is deduced from the transmissibility of the plasma sprayed coatings that, the bimodal distribution of microstructure will have an important influence on their mechanical properties. Because the plasma sprayed nanocoatings have typical layered structure, and possess a certain amount of unmelted nanoparticles, pores, microcracks and interface, the microhardness and fracture toughness values of the coatings exhibit obvious dispersion which can be analyzed by means of Weibull statistical analysis as follows[11]:

$$\ln\left\{\ln\left[\frac{1}{1-F}\right]\right\} = m\left[\ln(t) - \ln(T)\right] \qquad (3)$$

Where, F is the cumulative probability density function of each sample. m is the Weibull modulus which reflecting the dispersion of the data, and its value is inversely proportional to the dispersion. T is the characteristic value, which can reflect the average characteristics.

The experimental data of microhardness and fracture toughness of the coating sprayed at CPSP=437 were presented in Table 1, and the corresponding Weibull distribution plots were shown in Fig.6. As clearly seen from Fig. 6(a) that the Weibull curve fitted of the microhardness has two separate stages with different slopes, indicating that the microhardness of the coating possesses bimodal distribution, which corresponds to the existence of bimodal structure (PM and FM region) in the coating. Line A and line B show the hardness Weibull distribution of PM and FM region, respectively. Clearly, because PM region has retained partially melted powders and has a loose porous structure, the mean value of hardness (T_A=925) in PM region is lower than that (T=1299) in FM region. The slope of fitted line A is bigger, indicating that the hardness dispersity of PM region is lower, and the structure of PM region is more uniform. While the higher hardness dispersity of FM region is due to the pores, cracks, interface between the lamell and other defects in the

Table 1 Experimental data of microhardness and fracture toughness of Al_2O_3-13wt%TiO_2 nanocoatings plasma sprayed at CPSP=437

Region	Microhardness (HV_{100})	Fracture toughness, K_C/(MPa • $m^{1/2}$)
FM	1622, 1572, 1480, 1353, 1339, 1287, 1236, 1211, 1187, 1130, 1108, 1069	4.96, 5.12, 5.44, 5.65, 5.81, 5.93, 6.32, 6.49, 6.62, 6.89, 6.96, 7.12
PM	1010, 1002, 953, 941, 910, 896, 865, 823	7.54, 8.08, 8.24, 8.32, 8.53, 9.04, 9.52, 9.93

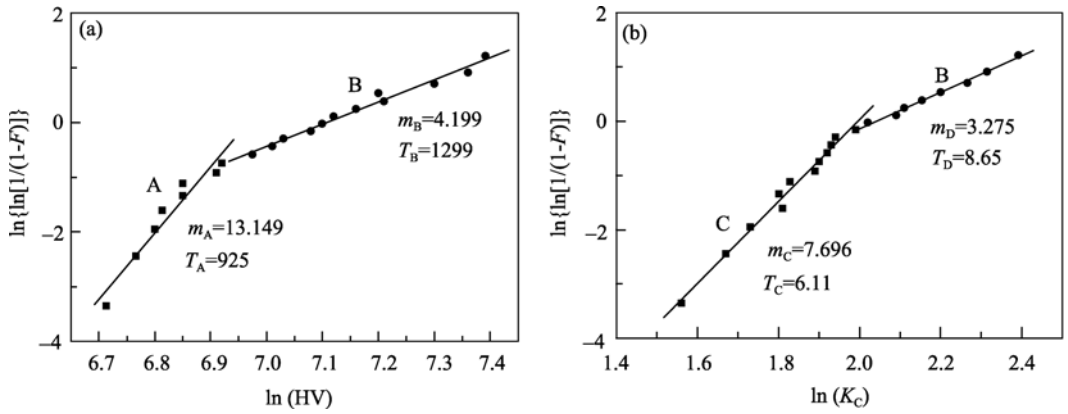

Fig. 6 Weibull plots of (a) microhardness and (b) fracture toughness of Al_2O_3-13wt%TiO_2 nanocoatings plasma sprayed at CPSP=437

coating.

The Weibull curve fitted of fracture toughness also has two separate stages with obvious different slopes, line C and line D represents the fracture toughness distribution of FM and PM region, respectively. As mentioned above, there are a large of nanostructure particles in PM region, furthermore, the interfaces between FM region and PM region are responsible for the significantly improved fracture toughness by crack deflection, trapping and arresting which improve the crack growth resistance[12-13]. Line D shows the mean fracture toughness of 8.65 MPa·$m^{1/2}$, which is higher than line C with that of 6.11 MPa·$m^{1/2}$. Meanwhile, the crack obstruction and deflection also increased the complexity and uncertainty of crack propagation path, and enhanced the toughness dispersity of PM region accordingly.

3 Conclusions

Nanostructured Al_2O_3-13wt% TiO_2 coatings were produced by plasma spraying agglomerated nanocrystalline powders, the following conclusions were drawn based on the investigation of microstructure and mechanical properties.

1) XRD patterns taken from all Al_2O_3-13wt%TiO_2 plasma sprayed coatings consist of α- and γ-Al_2O_3; peaks of the TiO_2 phase were not observed. It is evident that the phase composition of coatings is sensitive to the CPSP, and as the CPSP increases, the volume fraction of α-Al_2O_3 decreases and γ-Al_2O_3 begins to dominate the microstructure.

2) The microstructure of the coatings was found to present a bimodal distribution consisting of two distinct regions: one was fully-melted (FM) and quenched as γ-Al_2O_3 phase with the shape of lamellar splats, and the other was partially-melted (PM) with a particulate microstructure retained from the starting agglomerates. Moreover, the percentage of PM region, which is proportional to unmelted α-Al_2O_3 nanoparticles, decrease with an increase in the critical plasma spray parameter (CPSP) related to the temperature of the plasma torch and/or particle temperature.

3) The Weibull distribution analysis shows that the values of microhardness and fracture toughness of the coating present a bimodal distribution, which is correspond to the bimodal microstructure of the nanostructure coating. The mean value and the dispersity of microhardness of PM region is lower than that of FM region, but the mean value and the dispersity of fracture toughness of PM region are both higher than that of FM region.

Acknowledgements: The authors sincerely thank Engineer L. Wang for performance of the SEM observations, Dr. S. J. Liu for TEM, Engineer H. S. Wang for XRD, and Prof. X. Z. Li, Dr. X. G. Chen and Dr. A. Du for helpful discussions.

References:

[1] Dejang N, Watcharapasorn A. Fabrication and properties of plasma-sprayed Al_2O_3/TiO_2 composite coatings: a role of nano-sized TiO_2 addition. *Surface & Coatings Technology,* 2010 **204(9/10):** 1651–1657.

[2] Ye Y P. Microstructure and mechanical properties of yttria-stabilized ZrO_2/Al_2O_3 nanocomposite ceramics. *Ceramics International,* 2008, **34(8):** 1797–1803.

[3] Zhang J X, He J N, Dong Y C, *et al*. Microstructure and properties of Al_2O_3-13% TiO_2 coatings sprayed using nanostructured powders. *Rare Metals*, 2007, **26(4):** 391–397.

[4] Jordan E H, Gell M, Sohn Y H, *et al*. Fabrication and evaluation of plasma sprayed nanostructured alumina–titania coatings with superior properties. *Materials Science and Engineering* A, 2001, **301(1):** 80–89.

[5] Venkataraman R, Krishnamurthy R. Evaluation of fracture toughness of as plasma sprayed alumina–13wt% titania coatings by micro-

indentation techniques. *Journal of the European Ceramic Society*, 2006, **26(3):** 3075–3081.

[6] Lin X H, Zeng Y, Lee S W. Characterization of alumina–3wt% titania coating prepared by plasma spraying of nanostructured powders. *Journal of the European Ceramic Society*, 2004, **24(3):** 627–634.

[7] Song E P, Ahn J, Lee S. Effects of critical plasma spray parameter and spray distance on wear resistance of Al_2O_3-8wt% TiO_2 coatings plasma-sprayed with nanopowders. *Surface & Coatings Technology*, 2008, **202(3):** 3625–3632.

[8] Yılmaz R, Kurt A O, Demir A. Effects of TiO_2 on the mechanical properties of the Al_2O_3- TiO_2 plasma sprayed coating. *Journal of the European Ceramic Society*, 2007, **27(2):** 1319–1323.

[9] Zhang J X, He J N, Dong Y C, *et al*. Microstructure characteristics of Al_2O_3-13wt% TiO_2 coating plasma spray deposited with nanocrystalline powders. *Journal of Materials Processing Technology*, 2008, **197(1/2/3):** 31–35.

[10] Wang D S, Tian Z J. Microstructural characteristics and formation mechanism of Al_2O_3-13wt% TiO_2 coatings plasma-sprayed with nanostructured agglomerated powders. *Surface & Coatings Technology*, 2009, **203(10/11):** 1298–1303.

[11] Wei Z Y, Ye H. Microstructure and property of nanostructured Al_2O_3-13wt% TiO_2 coatings prepared by plasma spraying. *Transactions of Materials and Heattreatment*, 2009, **30(2):** 146–151.

[12] Luo H, Goberman D, Shaw L, *et al*. Indentation fracture behavior of plasma-sprayed nanostructured Al_2O_3-13wt% TiO_2 coatings. *Materials Science and Engineering*: A, 2003, **346(1/2):** 237–245.

[13] Pavitra B, Nitin P, Alexandre V. Improved interfacial mechanical properties of Al_2O_3-13wt% TiO_2 plasma-sprayed coatings derived from nanocrystalline powders. *Acta Materialia*, 2003, **51(10):** 2959–2970.

等离子喷涂纳米 Al_2O_3-13wt% TiO_2 涂层组织与性能的双态分布特性研究

路学成[1,2], 阎殿然[1], 杨 勇[1], 何继宁[1], 张建新[1], 董艳春[1]

(1. 河北工业大学 河北省新型功能材料实验室, 天津 300130; 2. 军事交通学院 装运机械系, 天津 300161)

摘 要: 采用由喷雾造粒制备的纳米团聚粉末并通过等离子喷涂制备出纳米 Al_2O_3-13wt% TiO_2 涂层. 研究分析了涂层的相组成、显微结构、硬度及断裂韧性, 结果发现, 该纳米涂层呈现出由两部分不同区域组成的双态分布结构: 一部分为完全熔化后凝固形成的层状结构; 另一部分则为部分熔化的粒状结构, 其内保留来源于喷涂喂料的纳米或亚微米粒子. 涂层中与未熔纳米 α-Al_2O_3 粒子含量成比例的部分熔化区百分数可以通过调整关键喷涂工艺参数(CPSP)来控制. 纳米涂层所具有的这种混合结构特性, 可以被其力学性能的双态分布特征所证实. Weibull 统计分析表明, 涂层的显微硬度和断裂韧性均呈现出双态分布, 部分熔化区的显微硬度及其分散性均比完全熔化区低, 而其断裂韧性及其分散性则均比完全熔化区高.

关 键 词: 等离子喷涂; 纳米涂层; 组织结构; 力学性能; 双态分布

中图分类号: TB383; TG174 **文献标识码:** A